Supplementary Information

Strain Induced Type-II Band Alignment Control in CdSe Nanoplatelets / ZnS Sensitized Solar Cells

Songping Luo[1⁄⁄], Miri Kazes[2⁄⁄], Hong Lin[1*] and Dan Oron[2]*

[1]State Key Laboratory of New Ceramics & Fine Processing, School of Material Science and Engineering, Tsinghua University, Beijing 100084, P.R. China

[2]Department of Physics of Complex Systems, Weizmann Institute of Science, Rehovot 76100, Israel

1. Morphology of electrodes

Figure S1 (a) shows the SEM images of bare TiO_2 and CdSe NPLs sensitized TiO_2 electrodes. It can be seen that the surface of TiO_2 particles become rough after the deposition of CdSe NPLs. Figure S1 (b) shows the elemental analysis of CdSe NPLs sensitized TiO_2 electrode with ZnS coating and the corresponding results are displayed in Table S1. It is reasonable that both the Cd/Se and Zn/S atomic ratios are approximate 1：1. These were characterized by field emission scanning electron microscope (FESEM: LEO 1530, Gemini, Zeiss, Germany) with an Energy Dispersive Spectroscopy (EDS) attachment. Figure S1(c) displays the photographs of front and back side of CdSe NPLs sensitized TiO_2 electrode and the sensitized electrode after ZnS coating. Judging from the color, the NPLs have penetrated into the porous TiO_2. The color then turned to brown after ZnS coating, due to the type-II indirect transition.

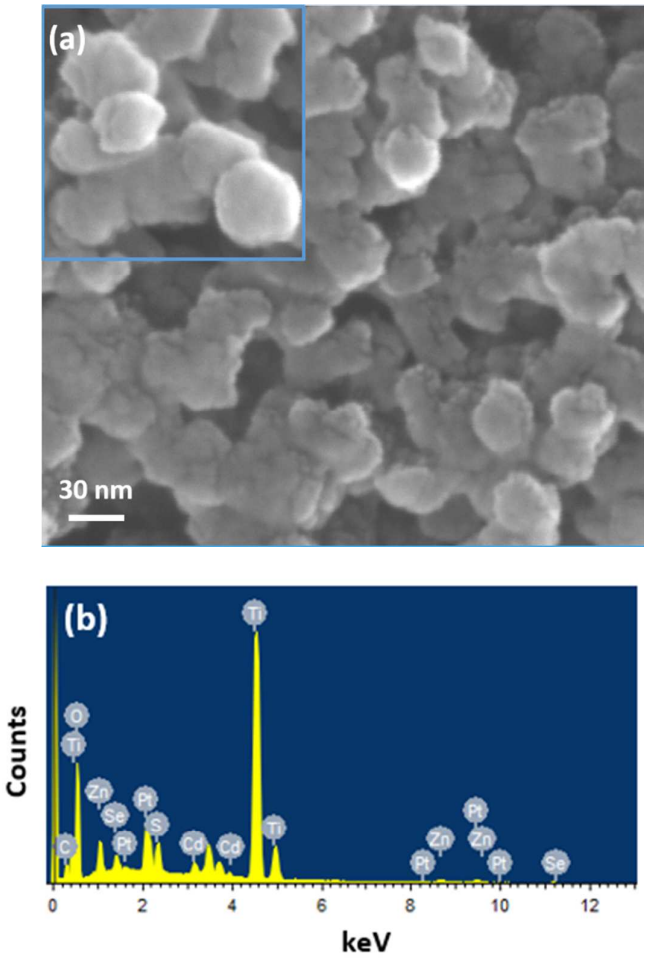

Figure S1. (a) SEM images of TiO_2 and CdSe NPLs sensitized TiO_2 electrodes, inset shows the SEM image of bare TiO_2 film. (b) Elemental analysis image of CdSe NPLs sensitized TiO_2 electrode with ZnS coating. (c) Photographs of CdSe NPLs sensitized TiO_2 and the sensitized films with ZnS coating.

Table S1. Elemental analysis results

Element	Mass ratio	Atomic percentage
C	3.02	7.31
O	32.40	58.89
S	1.90	1.72
Ti	45.52	27.63
Zn	4.50	2.00
Se	1.67	0.61
Cd	1.80	0.47
Pt	9.20	1.37
Total	100	

2. Raman spectra

Figure S2 shows the Raman spectra of bare TiO_2 and CdSe NPLs sensitized TiO_2 electrodes. The two kinds of photoelectrodes exhibit Raman peaks at 141 cm^{-1}, 201 cm^{-1}, 395 cm^{-1}, 513 cm^{-1}, 636 cm^{-1}, originating from anatase and rutile TiO_2.[1] Sensitization of CdSe NPLs lowered the intensity of the Raman peaks originating from TiO_2, especially the peak at 141 cm^{-1}. As previously reported, the Raman peak located at 289 cm^{-1} should be likely assigned to phonons of structure associated with the surface of CdSe NPLs. [18] It should be noted that the Raman peak intensity located at 201 cm^{-1} is also attributed to longitudinal (LO) phonon mode of CdSe NPLs,[2] that's

why the corresponding peak intensity of TiO_2/CdSe in contrast with peaks characteristic of the TiO_2 film alone.

3. Eg from Kubelka- Munk function

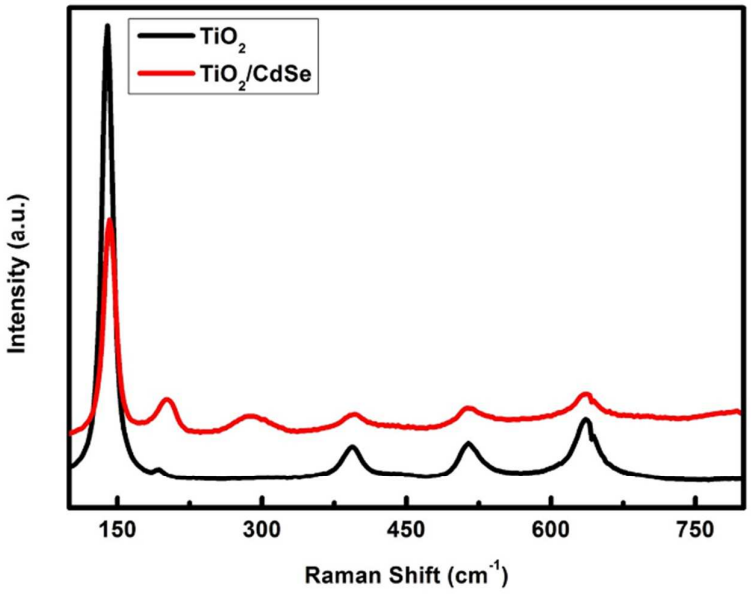

Figure S2. Raman spectra of bare TiO_2 and CdSe NPLs sensitized TiO_2 electrodes.

In this part, the relevant equations are as follows:[3]

$$F(\mathrm{R}) = \frac{(1-\mathrm{R})^2}{2R} = \frac{\alpha(\text{absorption coefficient})}{S(\text{sattering coefficient})} \quad (1)$$

$$\alpha \mathrm{h}\upsilon \propto (\mathrm{h}\upsilon - E_0)^{\mathrm{n}} \quad (2)$$

Where $\mathrm{h}\upsilon$ is the energy of the incident photon and E_0 is the optical absorption edge energy. The exponent (n) should be chosen as 1/2 or 2, depending on the type of samples' optical transition, direct or indirect optical transition, respectively. Here n was selected as 1/2 in that usually CdSe was termed as a direct-band-gap semiconductor. It is known that the scattering coefficient is weakly dependent on the

energy, and thus the absorption coefficient is proportional to F(R). Therefore, based on the intersection of abscissa axis with the tangent line of the $[F(\mathrm{R})\mathrm{h}\upsilon]^2 \sim \mathrm{h}\upsilon$ spectra, the band gaps can be determined.

4. Statistics of cell performances

Here we show the statistic results of cell performances. From the images below, it can be known that about half of the solar cells have achieved an open-circuit voltage (V_{oc}) above 600 mV. Short-circuit current density (J_{sc}) of 6~12 mA cm^{-2} was obtained by most solar cells. To some extent, the solar cells based on CdSe NPLs have succeeded in great progress upon high V_{oc} and J_{sc}.

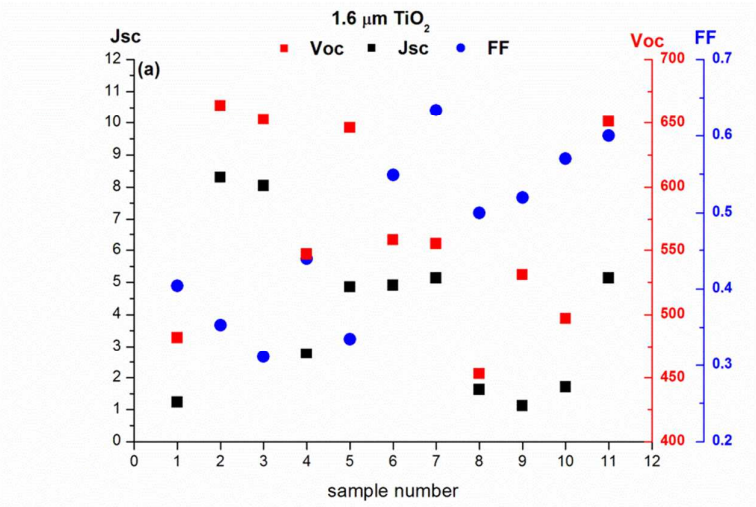

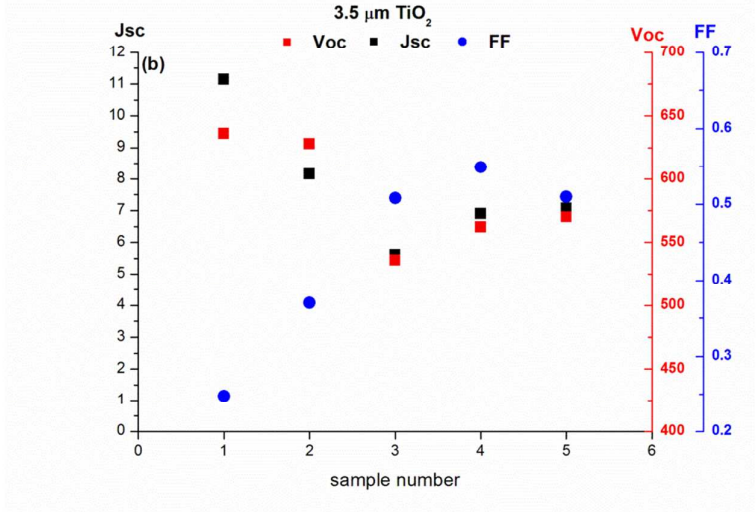

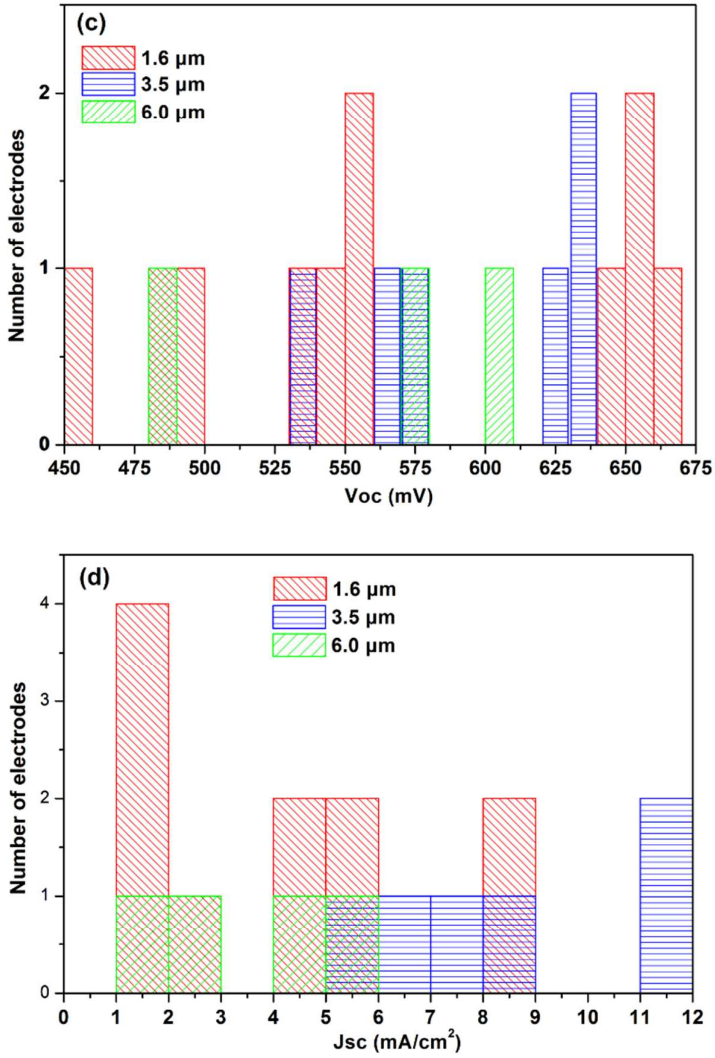

Figure S3. Statistic results of J_{sc}s , V_{oc}s and FFs of NPLs sensitized solar cells based on (a) 1.6 μ m and (b) 3.5 μ m TiO_2 films. Statistic results of (c) V_{oc}s and (d) J_{sc}s of NPLs sensitized solar cells based on TiO_2 films with different thicknesses.

5. Electrochemical Impedance Spectroscopy (EIS) analysis

EIS measurements were conducted to further study the charge transport process at the interface of photoanode and counter electrode with electrolyte. Figure S4 shows

the electrochemical impedance spectra of cells in the forms of Nyquist plots. Equivalent circuit model displayed in the inset was employed to fit the measured spectra to get the specific charge transport parameters, which are displayed in Table S2. In general, the Nyquist spectra of cells include two semicircles, the left one (high frequency region) and the right one (intermediate frequency region) corresponding to the charge transfer at the counter-electrode|electrolyte interface and TiO_2|sensitizer|electrolyte interfaces, respectively. Larger recombination resistance (R_{ct}) at the TiO_2| sensitizer |electrolyte interfaces signifies smaller recombination rate in the cells. Clearly, R_{ct} of CdSe/ZnS based solar cells is larger than that of CdSe based one, due to the CB energy barrier afforded by the ZnS layer. It is reasonable that R_{ct} decreases in CdSe/ZnSe based solar cells with thicker TiO_2 films, since it is longer path and takes longer time for the injected electrons in thicker TiO_2 film to be collected by FTO substrate, and thus creating more chances for electrons to recombine with the oxidized species in the electrolyte. Theoretically, there should be almost no difference in series resistances (R_s) and charge transfer resistances (R_{CE}) at the counter-electrode|electrolyte interface for all cells. However, the R_s and R_{CE} of 3.5 μm TiO_2/CdSe/ZnS based solar cells are slightly larger than those of other cells, probably due to accidental cell manufacturing process, which should be the reason for the relatively lower *FF*.

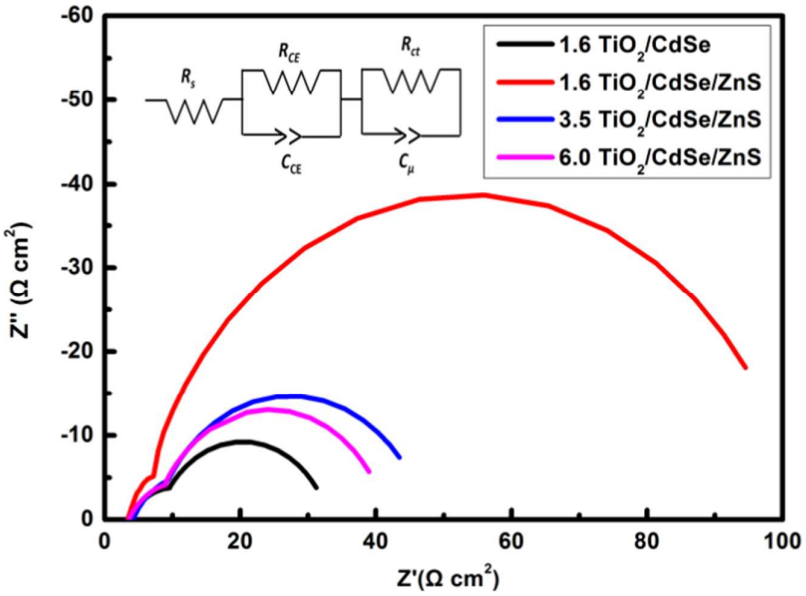

Figure S4. EIS spectra in Nyquist plots for the solar cells based on different photoanodes in the dark at an applied forward bias of −0.7 V (close to the V_{oc}). Inset is the Equivalent circuit for fitting EIS spectra, Rs: series resistance; R_{CE}: charge transfer resistance at the counter-electrode|electrolyte interface, R_{ct}, recombination resistance at the photoanode |electrolyte interfaces, C_{CE}: capacitance at the counter electrode; C_{μ}: chemical capacitance.

Table S2. $\boldsymbol{R_s}$, $\boldsymbol{R_{CE}}$, R_{ct} and C_{μ} derived from EIS fitting results.

Photoanode	$\boldsymbol{R_s}$(Ω cm^2)	$\boldsymbol{R_{CE}}$(Ω cm^2)	$\boldsymbol{R_{ct}}$ (Ω cm^2)	$\boldsymbol{C_{\mu}}$(mF cm^{-2})
1.6 μm TiO_2/CdSe	3.70	12.76	25.68	8.09
1.6 μm TiO_2/CdSe/ZnS	3.39	11.87	97.92	2.03
3.5 μm TiO_2/CdSe/ZnS	4.15	17.16	40.50	5.18
6.0 μm TiO_2/CdSe/ZnS	3.56	14.93	34.79	6.54

References:

(1) Melendres, C. A.; Narayanasamy, A.; Maroni, V. A.; Siegel, R. W., Raman Spectroscopy of Nanophase Tio2. *J. Mater. Res.* **1989**, 4, 1246-1250.

(2) Cherevkov, S. A.; Fedorov, A. V.; Artemyev, M. V.; Prudnikau, A. V.; Baranov, A. V., Anisotropy of Electron-Phonon Interaction in Nanoscale Cdse Platelets as Seen Via Off-Resonant and Resonant Raman Spectroscopy. *Phys. Rev. B* **2013**, 88, 041303(R).

(3) Barton, D. G.; Shtein, M.; Wilson, R. D.; Soled, S. L.; Iglesia, E., Structure and Electronic Properties of Solid Acids Based On Tungsten Oxide Nanostructures. *J. Phys. Chem. B* **1999**, 103, 630-640.